ELSEVIER

Surface Science 386 (1997) 322–327

surface science

Electrical conduction via surface-state bands

Shuji Hasegawa [a,*], Xiao Tong [b], Chun-Sheng Jiang [a,1], Yuji Nakajima [a], Tadaaki Nagao [a]

[a] *Department of Physics, School of Science, University of Tokyo, 7-3-1 Hongo, Bunkyo-ku, Tokyo 113, Japan*
[b] *CREST, Japan Science and Technology Corporation (JST), Kawaguchi Center Bldg., Hon-cho 4-1-8, Kawaguchi, Saitama 322, Japan*

Received 5 November 1996; accepted for publication 26 February 1997

Abstract

We will discuss a two-dimensional electron system originating from a surface-state band and especially its electronic transport properties. We have found a surface superstructure that has a highly conductive surface-state band, the Si(111)-$\sqrt{21}\times\sqrt{21}$R$\pm$10.89° structure, induced by adsorption of a 0.14-atomic-layer of Au or Ag onto a Si(111)-$\sqrt{3}\times\sqrt{3}$-Ag surface. Photoemission spectroscopies showed that this $\sqrt{21}\times\sqrt{21}$ structure had a highly dispersive surface-state band crossing over the Fermi level, while the surface space-charge layer was a depletion layer. It was then concluded that the observed excess surface conductance was due to the two-dimensional band of the surface electronic state. © 1997 Elsevier Science B.V.

Keywords: Angle-resolved photoemission spectroscopy; Silicon; Surface electrical transport; Surface structure; X-ray photoelectron spectroscopy

1. Introduction

In general, electronic states at surfaces are more or less different from those in the bulk because of abrupt interruption of the crystal periodicity and dangling bonds at the surfaces. These surface states play main roles in their properties as well as in atomic structural reconstructions. Especially, because the surface states are localized only near the topmost atomic layers, the electrons in these states provide an inherently two-dimensional electron system. In contrast to conventional two-dimensional electron-gas systems formed with bulk-state electrons confined by band bending at heterojunctions [1], the two-dimensional electron system in the surface-state band is expected to have novel properties correlating with surface-structural modifications.

For example, a clean Si(111) surface reconstructs into a 7×7 superstructure to reduce the number of the dangling bonds [2]. This dangling-bond state on each "adatom" has an unpaired electron, resulting in a half-filled, therefore metallic, surface-state band [3]. This band is actually detected by angle-resolved ultra-violet photoelectron spectroscopy (ARUPS), denoted "S_1" in Fig. 1a. This surface state is always detected at the Fermi level (E_F) at any emission angle, indicating negligible band-dispersion. This may be because the overlap integral between the neighboring dangling-bond states is so small that

* Corresponding author. Tel: (+81) 3 3812.2111 (ex) 4167; fax: (+81) 3 5689.7257; e-mail: shuji@phys.s.u-tokyo.ac.jp

[1] Present address: Surface and Interface Laboratory, The Institute of Physical and Chemical Research, Wako, Saitama, 351-01, Japan.

PII S0039-6028(97)00331-2

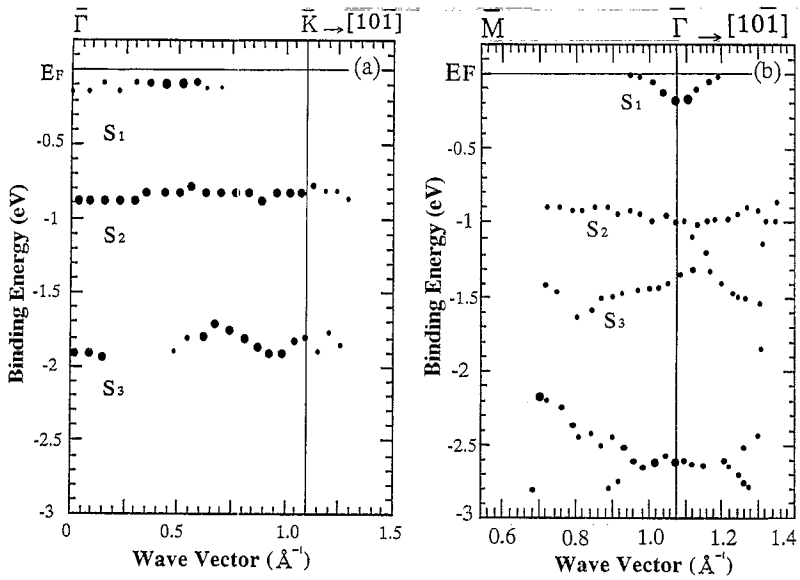

Fig. 1. Two-dimensional band-dispersion diagrams for (a) Si(111)-7×7 clean surface and (b) Si(111)-$\sqrt{3}\times\sqrt{3}$-Ag surface, respectively. Closed circles indicate the peak positions in ARUPS using unpolarized light from an He resonance lamp. Their sizes qualitatively correspond to the intensity of the respective peaks. The symbols $\bar{\Gamma}$, $\bar{M}$ and $\bar{K}$ are symmetric points in (a) 1×1 and (b) $\sqrt{3}\times\sqrt{3}$ surface Brillouin zones, respectively.

the electrons in the state are almost localized on the respective "adatoms". In this case, therefore, electrical conductivity through the dangling-bond-state band is not expected to be very high in spite of its metallic nature.

Let us consider another example, a Si(111)-$\sqrt{3}\times\sqrt{3}$-Ag surface, where Ag atoms of 1 monolayer (ML) are adsorbed to form covalent bonds with the substrate Si atoms, leaving no dangling bonds on the surface [4,5]. Thus an energy gap exists between the surface-state bands originating from bonding and anti-bonding states of surface-atom bonds [6]. These states are also observed in ARUPS measurements, denoted as "S_1" and "S_2", respectively, in Fig. 1b. We notice a peculiar feature in this band-dispersion diagram; the anti-bonding-state band S_1 is observed only in a narrow range of wave vectors around the $\bar{\Gamma}$ point and is highly dispersive. Furthermore, its bottom is located below E_F, so that some electrons are trapped in this band. Therefore, this situation is like a degenerate n-type semiconductor. This surface is thus expected to have higher electrical conductance in spite of its semiconducting nature, due to the excess electrons in the "surface conduction band S_1".

2. Experimental

We have measured the surface electrical conductance σ_S of the respective surfaces [7–9], using a linear four-probe method in ultrahigh vacuum [10]. In general, σ_S is composed of two contributions [11]; one is the conductance via surface-state bands σ_{SS} as described above, and the other is the conductance through a surface space-charge layer σ_{SC}; $\sigma_S=\sigma_{SS}+\sigma_{SC}$. In order to estimate the latter conductance σ_{SC}, we first have to measure the surface band bending or the position of the surface E_F. For this, we have measured Si 2p core-level shifts by X-ray photoelectron spectroscopy (XPS). We have then calculated the excess carrier concentration by solving the Poisson equation using the measured surface band-bending [12]. Finally, we can obtain σ_{SC} by multiplying the values of carrier mobilities in the bulk. In this way, the contribution of the space-charge layer σ_{SC} to the surface

conductance σ_S can be evaluated, and accordingly we can estimate σ_{SS} by subtracting σ_{SC} from the measured σ_S.

3. Results and discussion

The calculated σ_{SC} is shown as the solid curve in Fig. 2 as a function of the surface E_F position. The measured surface conductances σ_S are also plotted at the respective E_F positions at the respective surfaces. The E_F at the 7×7 surface is located around the middle of the band gap irrespective of the bulk doping [13], meaning a depletion layer of the surface space-charge layer. On the other hand, the E_F at the $\sqrt{3}\times\sqrt{3}$-Ag surface lies near the valence-band maximum [14], indicating a slight hole-accumulation layer. Therefore, the calculated σ_{SC} for the $\sqrt{3}\times\sqrt{3}$-Ag surface is higher than that

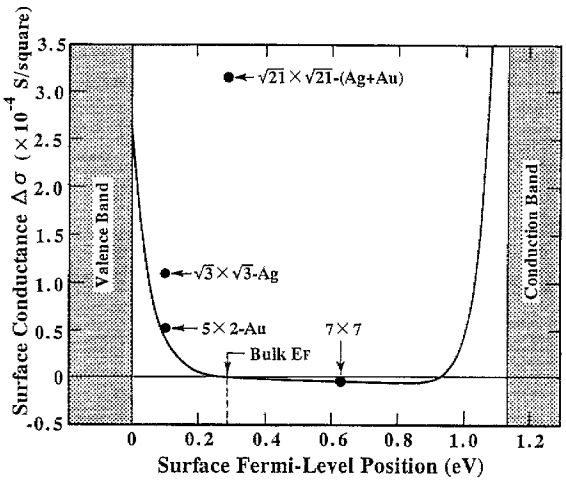

Fig. 2. The solid curve shows the excess electrical conductance through the surface space-charge layer σ_{SC} as a function of the surface Fermi-level position for a p-type silicon of 20 Ω cm resistivity at RT. This was calculated by solving the Poisson equation under given band bendings to obtain the excess carrier concentrations and then by multiplying them by the values of the carrier mobilities in the bulk. The electrical conductance under the flat-band condition was defined as the reference. The increases in conductance measured at the $\sqrt{3}\times\sqrt{3}$-Ag, 5×2-Au, and $\sqrt{21}\times\sqrt{21}$-(Ag+Au) surfaces with respect to the clean 7×7 surface are also plotted at the respective surface E_F positions. Such data points, especially for the $\sqrt{21}\times\sqrt{21}$ surface, are located above the solid curve σ_{SC}, which indicates extra conduction through the surface-state band σ_{SS}.

for the 7×7 surface. However, the measured σ_S was still higher; the data point is located slightly above the solid curve. This suggests a contribution of the excess conductance via the surface-state band of the $\sqrt{3}\times\sqrt{3}$-Ag surface [7]. More definite evidence for electrical conduction through a surface-state band has been obtained at a Si(111)-$\sqrt{21}\times\sqrt{21}$R$\pm10.89°$ surface [9]. The $\sqrt{21}\times\sqrt{21}$ superstructure appears by depositing additional Ag or Au atoms of ca 0.14 ML onto the $\sqrt{3}\times\sqrt{3}$-Ag surface. In the case of Ag deposition to induce the $\sqrt{21}\times\sqrt{21}$ structure, we had to cool the $\sqrt{3}\times\sqrt{3}$ substrate <250 K [8,15], although Au induced the $\sqrt{21}\times\sqrt{21}$ phase at room temperature [9]. When we measured the electrical conductance in situ during these depositions, the conductance showed remarkable increases, corresponding only to the formation of the $\sqrt{21}\times\sqrt{21}$ phases, as shown in Fig. 3. The conductance dropped again when the $\sqrt{21}\times\sqrt{21}$ phases disappeared with further depositions. The maximum conductances ca 0.14 ML coverages of additional Au are plotted in Fig. 2. The E_F position at this $\sqrt{21}\times\sqrt{21}$ structure induced by Au was measured by XPS and found to be located around the bulk E_F position. (We could not determine the E_F position at the $\sqrt{21}\times\sqrt{21}$ phase induced by additional Ag at lower temperatures because our XPS operated only at room temperature.) This means that the excess holes accumulated in the initial $\sqrt{3}\times\sqrt{3}$-surface-space-charge layer are depleted. The σ_{SC} should be thus decreased as shown by the solid curve in Fig. 2. On the contrary, the measured surface conductances σ_S are greatly enhanced at the $\sqrt{21}\times\sqrt{21}$ phase. On the other hand, 0.14 ML of additional Au adsorption on the $\sqrt{3}\times\sqrt{3}$-Ag surface is too small to form percolation paths on the two-dimensional triangular lattice [16]. We must then conclude that the remarkable enhancement of surface conductance is due to the contribution of the surface-state band of the $\sqrt{21}\times\sqrt{21}$ phase.

Next, we measured the ARUPS from the $\sqrt{21}\times\sqrt{21}$ surface induced by Au at room temperature (RT). Fig. 4 shows the spectra measured along the $[\bar{1}01]$ direction. The peaks indicated by small arrowheads, observed at emission angles θ_e ranging from 25 to 35°, are the same surface state

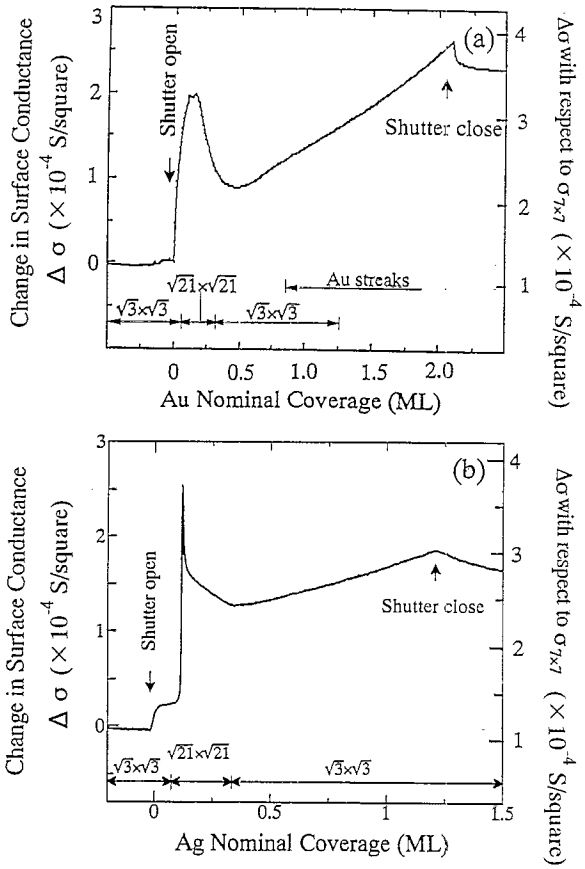

Fig. 3. Changes in surface conductance of Si(111)-$\sqrt{3}\times\sqrt{3}$-Ag surface during (a) Au deposition at RT, and (b) Ag deposition at 200 K. The Si wafer used was p-type with 20 Ω cm resistivity. The left ordinate shows the conductance increase from the initial $\sqrt{3}\times\sqrt{3}$-Ag surface, while the right ordinate indicates the conductance increase with respect to the clean 7×7 surface. The changes in surface structure in the course of the depositions, which were observed by reflection high-energy electron diffraction in separate runs of depositions, are also indicated.

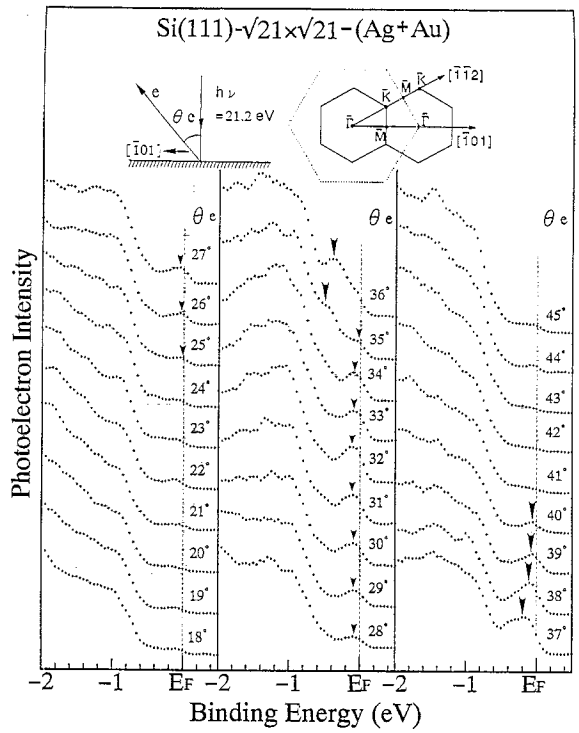

Fig. 4. ARUPS measured from the Si(111)-$\sqrt{21}\times\sqrt{21}$R10.89° surface, prepared by depositing 0.14 ML of Au onto the Si(111)-$\sqrt{3}\times\sqrt{3}$-Ag surface at RT. The electron analyzer was scanned in the [10$\bar{1}$] direction. Unpolarized UV light from a He resonance lamp was radiated on the surface with normal incidence. When we set the incident angle of the light to be off-normal, the peaks indicated by arrowheads were weakened.

as S_1 of the initial $\sqrt{3}\times\sqrt{3}$-Ag surface shown in Fig. 1b. However, the peaks indicated by big arrowheads, observed at emission angles θ_e ranging from 35 to 40°, newly appear only for the $\sqrt{21}\times\sqrt{21}$ surface. This new surface-state band also crosses over the E_F as the S_1 band of the $\sqrt{3}\times\sqrt{3}$ surface. We also notice a more important point; this intrinsic band of the $\sqrt{21}\times\sqrt{21}$ structure appears to be more highly dispersive so that the bottom of the band seems to overlap the bulk valence band. Thus we conclude that the very high surface conductance of the $\sqrt{21}\times\sqrt{21}$ structure comes from this newly formed metallic surface-state band. Because of two equivalent domains of the $\sqrt{21}\times\sqrt{21}$ phase with different azimuthal orientations by 21.8° relative to each other, we could not confirm the $\sqrt{21}\times\sqrt{21}$ symmetry of this new surface-state band. Although the character of this surface state is not yet clear, the $\sqrt{21}\times\sqrt{21}$ surface is the first example confirming electrical conduction via a surface-state band. In contrast to our macroscopic measurements of conductance, a nanometer-scale point contact using a scanning-tunneling-microscope tip has been employed to demonstrate the possible electrical conductance via the metallic dangling-bond state on the 7×7 surface [17]. However, the 7×7 surface did not seem to have excess surface conductance due to

the surface-state band in our macroscopic measurements.

As mentioned before, in order to form the $\sqrt{21} \times \sqrt{21}$ superstructure by additional Ag deposition, we had to cool the $\sqrt{3} \times \sqrt{3}$-Ag substrate <250 K. On warming up above 250 K, the $\sqrt{21} \times \sqrt{21}$ structure was destroyed and returned to the $\sqrt{3} \times \sqrt{3}$ structure; the additionally deposited Ag atoms were found to nucleate into three-dimensional islands on the $\sqrt{3} \times \sqrt{3}$ surface [8]. When additional Ag was deposited on the $\sqrt{3} \times \sqrt{3}$-Ag surface at RT, the Ag adatoms were found to form a two-dimensional-adatom gas phase below a critical coverage (~0.03 ML) [18]. "Adatom gas phase" refers to adatom monomers or clusters smaller than critical nuclei. These are extremely mobile on the $\sqrt{3} \times \sqrt{3}$-Ag surface because of very low activation barriers for surface migration. These mobile adsorbates do not nucleate unless their density exceeds some critical value (coverage). Such an adatom gas was found to greatly enhance the surface conductance. However, when the adatom coverage increased beyond the critical coverage, the gas phase began to nucleate into three-dimensional Ag islands and to be absorbed into them. This remarkably reduced the surface conductance [18]. Although the reason why the adatom gas phase enhances the surface conductance is not yet clarified, we expect some correlation to the $\sqrt{21} \times \sqrt{21}$ phase at lower temperatures, where the migration of Ag adatoms is suppressed to form the ordered structure for the gas phase.

In order to fully characterize the two-dimensional electron system in the $\sqrt{21} \times \sqrt{21}$-surface-state band, we are now preparing to separately measure the concentration and mobility of carriers in the band. However, these properties are expected to be influenced by extrinsic factors such as surface structural defects, for example, steps and domain boundaries. In fact, as revealed in scanning-tunneling-microscopy images of electron standing waves at steps on metal surfaces [19,20], the carriers in the surface-state band are severely scattered at the steps, resulting in reduction of the mobility. Yet the significance of carrier scattering by surface defects may be dependent on the Fermi wavelength of the carriers; the scattering can be unimportant for a surface-state band on a semiconductor. So it will be very interesting to investigate the correlation between the surface defects and the transport properties of the surface-state band. Quantum effects in electronic transport via the two-dimensional electron system in the surface-state band will also be fascinating, if any exist.

Acknowledgements

The results presented here have been obtained in collaboration with Dr Tomohide Takami, Mr Fumio Shimokoshi, Gen Uchida and Ms Sakura Takeda. We thank Professor Shozo Ino of the University of Tokyo for his valuable discussions. This work has been supported in part by a grant-in-aid from the Ministry of Education, Science, Culture, and Sports of Japan, and also by the CREST (Core Research for Evolutional Science and Technology) of the Japan Science and Technology Corporation (JST).

References

[1] For example, see special issues in Surf. Sci. 73 (1978); 98 (1980); 113 (1982); 142 (1984); 170 (1986); 196 (1988); 229 (1990).
[2] K. Takayanagi, Y. Tanishiro, M. Takahashi, S. Takahashi, J. Vac. Sci. Technol. A3 (1985) 1502; Surf. Sci. 164 (1985) 367.
[3] G.V. Hansson, R.I.G. Uhrberg, Surf. Sci. Rep. 9 (1988) 197; Critical Rev. Solid State Mater. Sci. 17 (1991) 133.
[4] Y.G. Ding, C.T. Chan, K.M. Ho, Phys. Rev. Lett. 67 (1991) 1454; Phys. Rev. Lett. 69 (1992) 2452.
[5] S. Watanabe, M. Aono, M. Tsukada, Phys. Rev. B 44 (1991) 8330.
[6] L.S.O. Johansson, E. Landemark, C.J. Karlsson, R.I.G. Uhrberg, Phys. Rev. Lett. 63 (1989) 2092; Phys. Rev. Lett. 69 (1992) 2451.
[7] C.-S. Jiang, S. Hasegawa, S. Ino, Phys. Rev. B 54 (1996) 10389.
[8] X. Tong, S. Hasegawa, S. Ino, Phys. Rev. B 55 (1997) 1310.
[9] C.-S. Jiang, X. Tong, S. Hasegawa, S. Ino, Surf. Sci. 376 (1997) 69.
[10] S. Hasegawa, S. Ino, Phys. Rev. Lett. 68 (1992) 1192; Surf. Sci. 283 (1993) 438; Thin Solid Films 228 (1993) 113; Int. J. Mod. Phys. B 7 (1993) 3817; H. Sakaki, H. Noge (Eds.), Nanostructures and Quantum Effects, Springer, Berlin, 1994, p. 104.

[11] M. Henzler, in: J.M. Blakely (Ed.), Surface Physics of Materials I, Academic Press, New York, 1975, p. 241.
[12] C.E. Young, J. Appl. Phys. 32 (1961) 329.
[13] F.J. Himpsel, G. Hollinger, R.A. Pollack, Phys. Rev. B 28 (1983) 7014.
[14] S. Kono, K. Higashiyama, T. Kinoshita, T. Miyahara, H. Kato, H. Ohsawa, Y. Enta, F. Maeda, Y. Yaegashi, Phys. Rev. Lett. 58 (1987) 1555.
[15] Z.H. Zhang, S. Hasegawa, S. Ino, Phys. Rev. B 52 (1995) 10760.
[16] R. Schad, S. Heun, T. Heidenblut, M. Henzler, Phys. Rev. B 45 (1992) 11430.
[17] Y. Hasegawa, I.-W. Lyo, Ph. Avouris, Appl. Surf. Sci. 76/77 (1994) 347.
[18] Y. Nakajima, G. Uchida, T. Nagao, S. Hasegawa, Phys. Rev. B 54 (1996) 14134.
[19] Y. Hasegawa, Ph. Avouris, Phys. Rev. Lett. 71 (1993) 1071.
[20] M.F. Crommie, C.P. Lutz, D.M. Eigler, Nature 363 (1993) 524.